Multiple beam Michelson-based interferometer

Article *in* Optical Engineering · August 2009
DOI: 10.1117/1.3192784

Multiple beam Michelson-based interferometer

David Sánchez-de-la-Llave
Sabino Chávez-Cerda
Instituto Nacional de Astrofísica, Óptica,
y Electrónica
Coordinación de Óptica
Apartado Postal 51
Puebla, Puebla 72000
México
E-mail: dsanchez@inaoep.mx

Marcelino Anguiano-Morales
Centro de Investigaciones en Óptica
Loma del Bosque No 115
Col. Lomas del Campestre
León, Guanajuato 37150
México

D. Ramirez-Martinez
Marcela Maribel Méndez-Otero
Marcelo David Iturbe-Castillo
Benemérita Universidad Autónoma de Puebla
Av. San Claudio y Río Verde
Puebla, Puebla 72000
México

Abstract. We present a modification to the classic Michelson interferometer that allows the interference of multiple beams with equal amplitude. The proposed architecture presents the same advantages and simplicity as those of a classic Michelson interferometer. The basic unit of the device consists of a beamsplitter and two mirrors arranged as in a Michelson interferometer. To increase the number of interfering beams, the mirrors are replaced by a basic unit. In order to demonstrate the type of interference patterns that can be obtained, we present interferograms corresponding to three to eight interfering beams. The system can be used to optically induce photonic lattices. [DOI: 10.1117/1.3192784]

Subject terms: interferometry; interferometers; waveguides; photonics.

Paper 090060R received Jan. 28, 2009; revised manuscript received Jun. 8, 2009; accepted for publication Jun. 12, 2009; published online Aug. 26, 2009.

1 Introduction

Transverse variations of a material refractive index can drastically modify the propagation of a beam traveling through such media. These variations can be optically induced in adequate nonlinear materials, creating photonic lattices where their features can be tuneable.[1] One-dimensional photonic lattices have been created using interference of two beams, whereas two-dimensional photonic lattices have been created using interference of three beams. Other types of lattice geometries, different from those obtained by interference, have been studied in the past.[2–5] However, lattices that can be obtained by optical interference are the most attractive. Classic interferometers combine two beams in order to obtain their corresponding interference pattern. Interferometric systems that allow for multiple-beam superposition have been proposed in the past.[6] An example is the interferometer of Jamin, which can be modified in such a way that it is possible to obtain interference of three beams.[7] In this architecture, controlling the phase and amplitude of the beams is a complicated task. However, interferometers that superpose more than four beams, where one can modify individually each beam phase and amplitude, have not been proposed in the past to the authors' best knowledge.

In this paper, we describe a multiple-beam interferometer based on the Michelson interferometer capable of superposing more than two beams with equal intensity. The direction of propagation of each of the interfering beams can be readily controlled.

0091-3286/2009/$25.00 © 2009 SPIE

2 Description of the Proposed Interferometer

A typical Michelson interferometer consists of one beamsplitter and two mirrors in a configuration like the one shown in Fig. 1. The beamsplitter divides the incident beam into two orthogonal beams that are reflected back by the mirrors and then recombined by the beamsplitter. The superposition of the recombined beams forms an interferogram when the field intensity is detected. In our proposal, depending on the desired number of beams to interfere, each mirror in the Michelson architecture is replaced by another Michelson interferometer (i.e., one 50/50 beam-

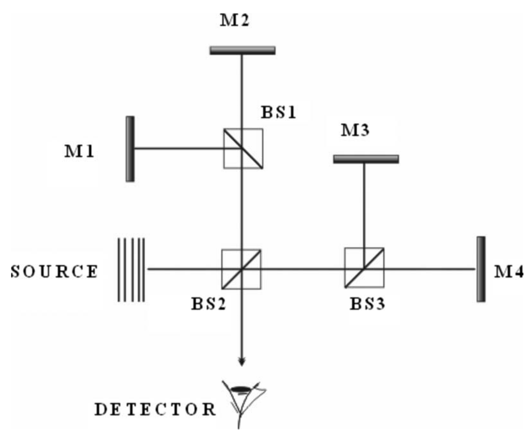

Fig. 1 Experimental setup for the interference of four fields, the source is a He–Ne laser. With this setup, one can obtain four independent beams with the same intensity at the output of the interferometer.

splitter and two mirrors). Hence, when one of the mirrors in the classical Michelson architecture is replaced by another Michelson interferometer, one obtains the superposition of three beams. In this case, the superposed beams do not have equal intensity. However, if both mirrors in the classical Michelson architecture are replaced each one by another Michelson interferometer, then, at the output of the device, four equally intense beams will be superposed. Repeating this procedure once more (i.e., replacing all mirrors by Michelson interferometers), the architecture contains eight mirrors leading to the interference pattern of eight beams of equal amplitude. Thus, the maximum number of interfering beams that can be obtain is given by 2^{n+1}, where n is the number of times the interferometer is modified by replacing its mirrors by beamsplitters. Because each mirror controls the phase of one beam, it is possible to readily control the phase of each of the interfering beams. Replacing mirrors by beam stops allows us to have any number, $<2^{n+1}$, of interfering beams at the interferometer output. A limited version of this idea was used to obtain an optical vortex array generator.[8]

3 Interference of Multiple Plane Waves

Consider that the beams obtained from the proposed interferometer have plane wavefronts. Interference of three plane waves or more can produce periodic or quasiperiodic transversal or longitudinal distributions. Invariant distributions can be obtained when the wave vectors of the interfering beams are arrayed over a circle. If this is not the case, then a dependence of the pattern with the coordinate z is present. In order to illustrate this situation, consider two plane waves with wave vectors over the x-z plane of the form

$$U_1 = \exp[-i(kx \sin \alpha + kz \cos \alpha)],$$

$$U_2 = \exp[-i(kx \sin \varphi + kz \cos \varphi)], \tag{1}$$

where α and φ are the angles with respect to the z-axis. The superposition of such beams produces an intensity pattern of the form

$$I = 2\{1 + \cos[kx(\sin \alpha - \sin \varphi) + kz(\cos \alpha - \cos \varphi)]\}. \tag{2}$$

If we make $x=0$, then the intensity along the z-axis is given by

$$I = 2\{1 + \cos[kz(\cos \alpha - \cos \varphi)]\}. \tag{3}$$

It is clear from the last expression that the dependence with z disappears when the wave vectors are symmetric with respect to the z-axis. The same behavior is obtained when more than two beams are considered. As an illustrative example, consider the case of three plane waves with the same wavenumber and unit amplitude. The complex amplitude describing each beam can be described by

$$U(x,y,z) = \exp[-i(k_{xj}x + k_{yj}y + k_{zj}z)], \tag{4}$$

where k_{xj}, k_{yj}, and k_{zj}, represent the wave-vector components along the x, y, and z directions, respectively, and j is a number that differentiates the three waves. The interference of three plane waves can be described by

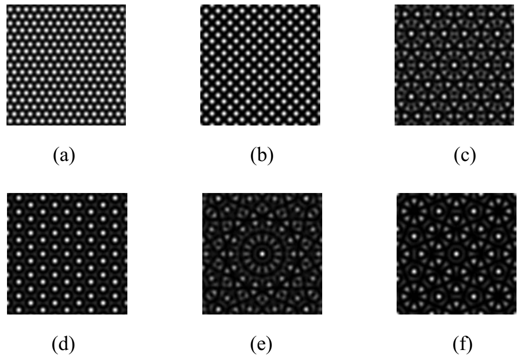

Fig. 2 Numerically obtained interference patterns for (a) three, (b) four, (c) five, (d) six, (e) seven, and (f) eight plane waves with wave vectors over a circle and relative phase of 0 rad between them.

$$\begin{aligned} I &= |\exp(ia) + \exp(ib) + \exp(ic)|^2 \\ &= 3 + 2\cos(a-b) + 2\cos(a-c) + 2\cos(b-c), \end{aligned} \tag{5}$$

where a, b, and c represent the phase of each wave. For three arbitrary plane waves described by Eq. (4), we can write

$$a = k_{x1}x + k_{y1}y + k_{z1}z,$$

$$b = k_{x2}x + k_{y2}y + k_{z2}z,$$

$$c = k_{x3}x + k_{y3}y + k_{z3}z. \tag{6}$$

Hence, the interfering pattern inside the volume where the three waves overlap is given by

$$\begin{aligned} I = 3 &+ 2\cos[(k_{x1}-k_{x2})x + (k_{y1}-k_{y2})y + (k_{z1}-k_{z2})z] \\ &+ 2\cos[(k_{x1}-k_{x3})x + (k_{y1}-k_{y3})y + (k_{z1}-k_{z3})z] \\ &+ 2\cos[(k_{x2}-k_{x3})x + (k_{y2}-k_{y3})y + (k_{z2}-k_{z3})z]. \end{aligned} \tag{7}$$

From Eq. (7), it is clear that the condition that must be fulfilled in order to obtain an invariant interference pattern along the z-axis is $k_{z1}=k_{z2}=k_{z3}$. Therefore, nondiffracting patterns are observed in planes perpendicular to the z-axis if the interfering plane waves have the same wavenumber and the same wave vector component along the z-axis.

In the following analysis, we are going to consider only wave vectors whose projection over the k_x, k_y plane falls over the perimeter of a circle, i.e.,

$$\vec{k} = (k_x, k_y) = k(\cos\theta, \sin\theta), \tag{8}$$

where θ is an integer multiple of the angle $\Theta = 2\pi/M$, where M is the number of waves to interfere and k is the wavenumber. In Fig. 2, we present numerical simulations of the interference patterns obtained when three to eight beams are superposed, without a relative phase delay between the beams. The beams wave vectors are equally spaced over the circle's perimeter. In the case of three waves, an interference pattern of bright circular spots in a hexagonal array is obtained. For the case of four waves, the interference pattern presented bright spots in a square array. The interference of five waves produced a pattern with a

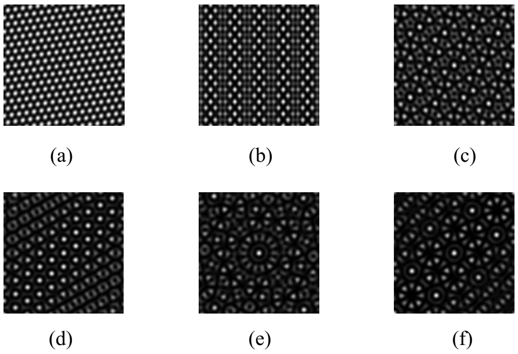

Fig. 3 Numerically obtained interference patterns for (a) three, (b) four, (c) five, (d) six, (e) seven, and (f) eight plane waves when one of the wave vectors is not over the circle.

central bright spot surrounded by a dark ring and more bright spots in a pentagonal array. Superposition of six waves produced a pattern similar to that obtained with three waves, but in this case, each bright spot is surrounded by a dark ring and a nonzero intensity region separates each bright spot. Interference of seven waves produced a pattern with a central bright spot surrounded by one bright ring. This pattern was similar to that obtained by the superposition of eight waves. The addition of more plane waves with wave vectors over the circle's perimeter must produce a pattern close to that of a Bessel beam (i.e., a central high-intensity bright spot surrounded by rings). As expected, the interference pattern is very sensitive to changes in the direction and phase of the interfering beams.

In Fig. 3, we present numerical simulations of the intensity distribution obtained when one of the wave vectors is not over the circle's perimeter. The less sensitive case is the one corresponding to the interference of three waves. When one wave vector is not over the circle's perimeter, the pattern presented some inclination and the bright spots were not circular. Taking into account Eq. (6) and an observation plane $z=0$, the phases of the waves considered in the nondiffracting case [Fig. 2(a)] can be written as

$$a = k_x x + k_y y,$$

$$b = -k_x x - k_y y,$$

$$c = k_y y. \tag{9}$$

Hence, the corresponding interference pattern is given by

$$I = 3 + 2\cos(2k_x x) + 2\cos(k_x x - 2k_y y) + 2\cos(k_x x + 2k_y y). \tag{10}$$

The pattern obtained in Fig. 3(a) was obtained by modifying the phase b as

$$b = -(k_x - \Delta)x - (k_y - \Delta)y, \tag{11}$$

i.e., the wave-vector components along the x and y directions were reduced by a constant amount Δ, maintaining the wavenumber constant and thus increasing the wave-vector component along the z direction. The expression describing the interference pattern under these conditions can be written as

$$I = 3 + 2\cos[(2k_x - \Delta)x + \Delta y] + 2\cos[k_x x - 2k_y y] + 2\cos[(k_x - \Delta)x + (2k_y - \Delta)y]. \tag{12}$$

Comparing Eqs. (12) and (10), one can observe that the second term at the right-hand side of Eq. (12) depends on both x and y, whereas in Eq. (10), it only depends on x. This situation accounts for the inclination of the pattern shown in Fig. 3(a) with respect to the one shown in Fig. 2(a). Regarding the fourth term at the right-hand side of Eq. (12), one can observe that different constants are multiplying the x and y variables, compared to the ones in the corresponding term in Eq. (10). Therefore, the bright spots shape is modified in Fig. 3(a) compared to the shape shown in Fig. 2(a). In the case of four beams, the misalignment produced a modulation that changes dramatically the interference patterns. For five waves, the central bright spot cannot be identified. For six waves, the pattern presented a

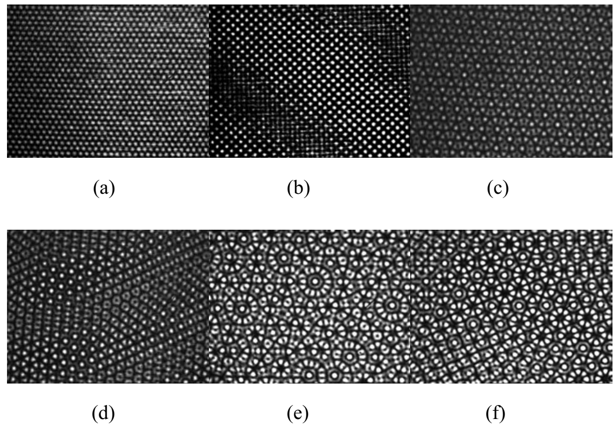

Fig. 4 Experimentally obtained interference patterns for (a) three, (b) four, (c) five, (d) six, (e) seven, and (f) eight beams from the multiple beam Michelson interferometer.

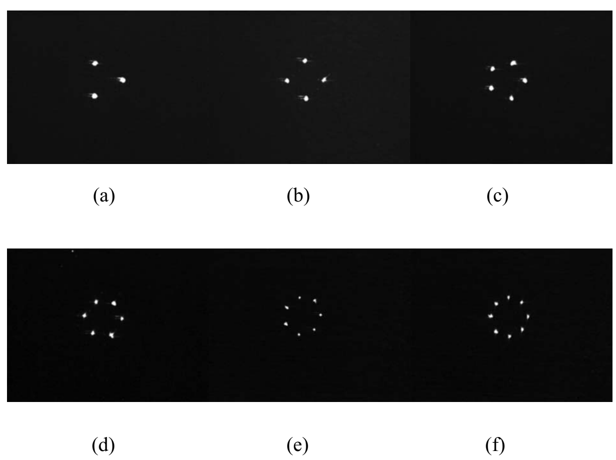

Fig. 5 Intensity of the optically obtained Fourier transform of the fields corresponding to the interference patterns shown in Fig. 4: (a) three beams, (b) four beams, (c) five beams, (d) six beams, (e) seven beams, and (f) eight beams.

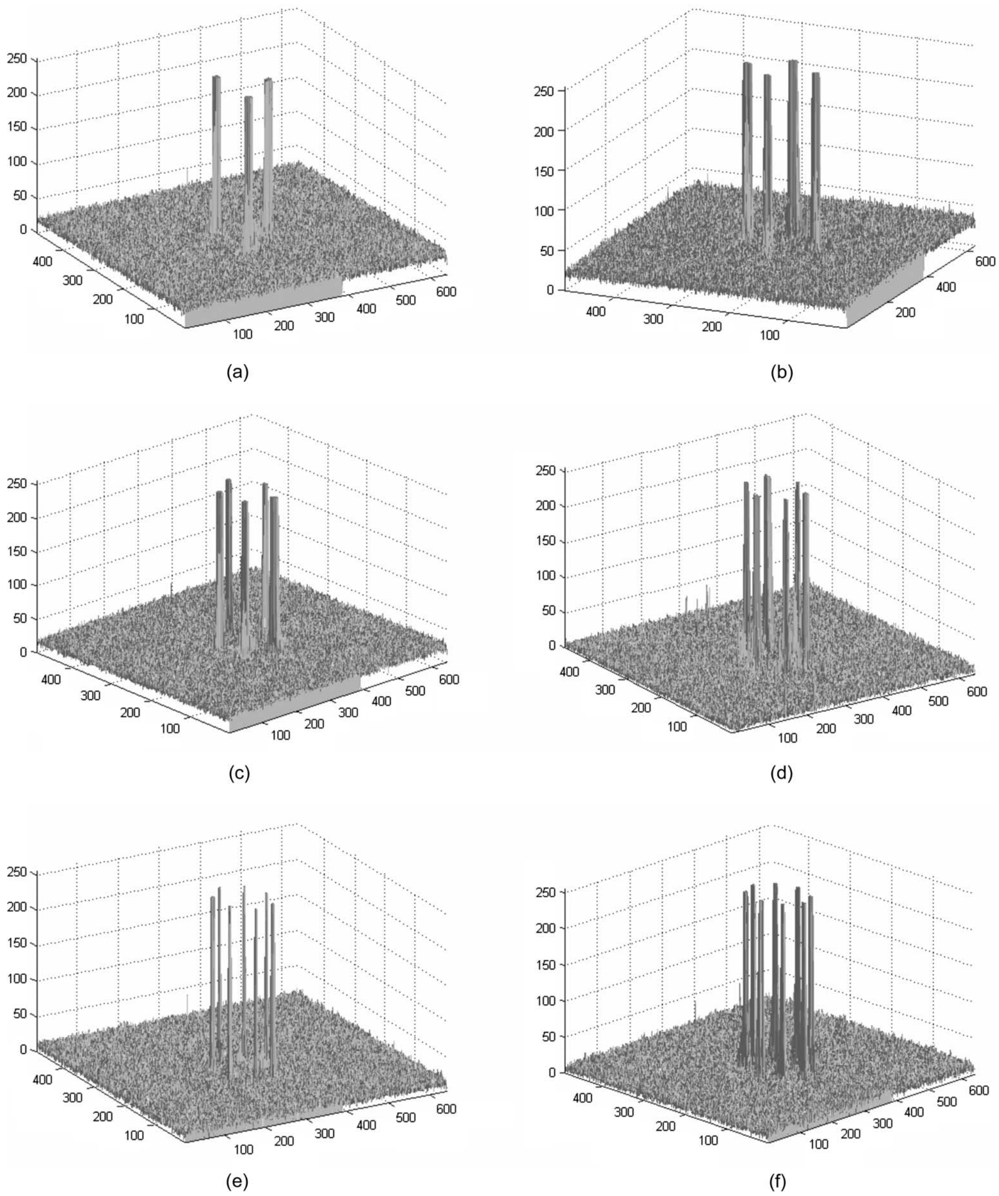

Fig. 6 Three-dimensional representation of the output field optical Fourier transform intensity; the output field consists of the superposition of (a) three, (b) four, (c) five, (d) six, (e) seven, and (f) eight beams.

change from circular to square bright spots with a hole in the center. Superposition of seven and eight beams produced patterns very similar to those obtained with all the wave vectors falling over the circle's perimeter; however, these patterns change with the distance z. As is shown by the numerical examples illustrated above, with this architecture one can implement a great variety of three-dimensional field structures. The output field can be employed to synthesize photonic lattices and/or waveguide arrays that are constant or variant along the field propagation direction. Also, the output of this interferometer can be used to illuminate one optical element or system in order to generate other type of intensity distributions.

4 Experimental Setup and Results

A 30-mW He–Ne laser beam at $\lambda = 633$ nm was filtered, expanded, and collimated to a diameter of 2 cm using a microscope objective and a lens. This beam illuminated a modified Michelson interferometer with seven 50/50 cube beamsplitters and eight mirrors, obtaining eight equal amplitude beams. The beams that were not used were blocked. Both the beamsplitters and the mirrors were set in optical mounts with fine movement, where it was possible to change the tilt in the x and y directions.

Experimental results for the superposition from three to eight beams are shown in Fig. 4. In the case of three beams, a very similar pattern to that obtained with perfect wave vector alignment was obtained. For four beams, the pattern obtained presented a modulation similar to that shown in Fig. 3(b). Something similar occurred for the interference of five beams, where it was not possible to identify the central bright spot obtained in the case of perfect wave vector alignment, but the distribution is close to that shown in Fig. 3(c). Interference of six beams produced a pattern that changes in all directions; only in some areas of the image is it possible to identify the characteristic bright spots of this case. Interference of seven and eight beams produced more complicated patterns than those obtained assuming one wave-vector mismatch; in both cases, we had misalignment in more than one wave. It is worthy noting here that the experimental implementation of the technique is limited regarding the number of beams that can be interfered. This limitation comes from the input beam and optics dimensions. As the number of beams increases, the angle they make with respect to the optic axis must be reduced; otherwise, some of them might escape from the setup and not interfere with the other beams at the output plane of the device. By Fourier transforming the field at the output plane of the device, one can detect the projection of the wave vectors over the k_x-k_y plane. This operation can be readily obtained optically by placing a lens a focal length from the interferometer output plane and detecting the field intensity at the lens focal plane. Adding a lens to the proposed architecture allows the user to control, in real time, the propagation direction of the interfering plane waves. The propagation direction of each plane wave is manifested at the lens Fourier plane by the spatial location of the point-like structure corresponding to each beam Fourier transform, and hence, modifications to the desired propagation direction can be controlled by observing the intensity distribution at the lens Fourier plane. The intensities of the optical Fourier transform of the fields corresponding to the interference patterns shown in Fig. 4 are depicted in Fig. 5. As it can be observed, small deviations in the propagation direction of the beams can produce noticeable changes in the obtained interference pattern. In Fig. 6, three-dimensional profiles of the output field optical Fourier transform intensity are shown.

5 Conclusion

In this work, we describe a modification to the Michelson interferometer that allows obtaining independent and equal intensity beams when the mirrors of the interferometer are substituted by another Michelson interferometer. This procedure can be repeated in order to obtain more beams. Numerical simulation and experimental results were obtained for the case of interference of three to eight plane waves. The numerical simulations considered beams with wave vectors arrayed over a circle. The case of one beam not having its wave vector over the circle was also simulated. The experimental results presented do not have all wave vectors arrayed over a circle. In our experimental setup, optical mounts with higher precision are required in order to obtain all wave vectors arrayed over a circle. However, the functionality of the proposed architecture (i.e., to superpose several beams of equal amplitude) was demonstrated. We also present a simple method that allows the user to control, in real time, the propagation direction of each of the beams that conforms the interference pattern. The proposed system can be used for the optical generation of photonic lattices and waveguide arrays.

References

1. J. W. Fleischer, M. Segev, N. K. Efremidis, and D. N. Christodoulides, "Observation of two-dimensional discrete solitons in optically induced nonlinear photonic lattices," *Nature* **422**, 147–150 (2003).
2. N. K. Efremidis, S. Sears, D. N. Christodoulides, J. W. Fleischer, and M. Segev, "Discrete solitons in photorefractive optically induced photonic lattices," *Phys. Rev. E* **66**, 046602 (2002).
3. J. W. Fleischer, T. Carmon, M. Segev, N. K. Efremidis, and D. N. Christodoulides, "Observation of discrete solitons in optically induced real time waveguide arrays," *Phys. Rev. Lett.* **90**, 023902 (2003).
4. D. Neshev, E. Ostrovskaya, Y. Kivshar, and W. Krolikowski, "Spatial solitons in optically induced gratings," *Opt. Lett.* **28**, 710–712 (2003).
5. H. Martin, E. D. Eugenieva, Z. Chen, and D. N. Christodoulides, "Discrete solitons and soliton-induced dislocations in partially coherent photonic lattices," *Phys. Rev. Lett.* **92**, 123902 (2004).
6. C. Roychoudhuri, "Multiple-beam interferometers," in *Optical Shop Testing*, 2nd ed., D. Malacara, Ed., pp. 207–245, Wiley, Hoboken, NJ (1992).
7. P. Hariharan and D. Sen, "Three-beam interferometer," *J. Sci. Instrum.* **36**, 70–72 (1959).
8. S. Vias and P. Senthilkumaran, "Interferometric optical vortex generator," *Appl. Opt.* **46**, 2893–2898 (2007).

David Sánchez-de-la-Llave is a researcher in the Optics Department at the National Institute for Astrophysics, Optics, and Electronics (INAOE) in México. He received his doctoral degree in engineering from the University of Massachusetts Lowell in 1998. His research interests are related to the field of optical information processing.

Sabino Chávez-Cerda received his PhD in nonlinear optics (physics) at Imperial College of Science and Technology, University of London. He has been a full-time researcher at INAOE since January 1995. His research field is theoretical linear and nonlinear optics, and he is investigating the physics of light propagation (as beams and pulses) in dispersive linear and nonlinear refractive media using analytical and numerical techniques.

Marcelino Anguiano-Morales received a degree in physics in 1999 from Facultad de Ciencias Física Matemáticas of the Benemérita Universidad Autónoma de Puebla (BUAP) México, and his master's degree in 2002. He received his PhD from INAOE in 2007. His research interests are the applications of invariant beams.

D. Ramirez-Martinez concluded her studies in physics in 2003 and her master's degree in 2006, in the Facultad de Ciencias Físico Matemáticas of the Benemérita Universidad Autónoma de Puebla, México. She is currently studying her doctoral degree in the same institution focused in the area of photonics. Her area of research is the generation of spatial solitons.

Marcela Maribel Méndez-Otero received a degree in physics in 1995 from the Facultad de Ciencias Física Matemáticas of the BUAP Mexico. Her master's and doctoral degrees were obtained in 1996 and 2000, respectively, at INAOE. She is currently working in the Facultad de Física Matemáticas. Her research involves measurement of nonlinear absorption and refraction in solid and liquid materials. Recently, she has initiated work on the propagation of invariant beams in free space. She is a full-time researcher at BUAP.

Marcello David Iturbe-Castillo is a titular researcher in the optics department at INAOE. He received his PhD from the same institute in 1996. His research interests are in nonlinear optical characterization of materials and propagation-invariant beams in linear and nonlinear media.